In-door occupancy survey of the 2.4 GHz band

Tomaž Šolc
Jožef Stefan International Postgraduate School
Jamova 39, 1000 Ljubljana, Slovenia
tomaz.solc@ijs.si

***Abstract*—The assumption that current unlicensed bands are overused is instrumental in the effort for opening up more spectrum to license-free consumer devices. While many studies have been made on the overall spectrum occupancy, few have focused specifically on the usage of unlicensed bands in environments common for consumer devices. To improve this situation we have performed an in-door survey of the 2.4 GHz frequency band in 5 different residential and 1 conference location in Slovenia between April and June 2014. In this paper we present a portable and robust device used for the measurements, describe the methodology for data analysis and show results from 6 short-term and 1 long-term measurement campaigns.**

I. Introduction

Recently there has been a growing interest into opening new frequency bands to unlicensed devices and secondary usage. The most well known of which is perhaps the UHF broadcast band and the opening of the so-called TV white-spaces. The common reason given for this effort is scarcity of available spectrum. With ever-increasing usage of consumer wireless technologies, the unlicensed frequency bands are assumed to be overcrowded. On the other hand, studies show that bands licensed for exclusive use remain relatively unused[1][2][3].

There have been plenty of occupancy studies that covered large parts of usable spectrum (e.g. 30 MHz to 3 GHz), but fewer studies focused on the unlicensed bands[4]. This is surprising, since technology-wise, users of the unlicensed spectrum evolve much faster than users encumbered by radio licenses from regulatory bodies. 100 MHz of spectrum between 2.4 and 2.5 GHz that forms the international industrial-scientific-medical (ISM) band is arguably the most ubiquitous range of frequencies employed by low-cost consumer devices. Given the extremely fast product cycle of such devices, it is unlikely that a 10 year old study of the situation in the 2.4 GHz band is still applicable today.

Existing studies also mostly focus on out-door measurements from a high ground to cover as much area as possible with the spectrum sensor. For consumer devices like wireless LAN connected laptops and smartphones however, spectrum occupancy in in-door environments is just as important.

We have heard plenty of anecdotal evidence that devices operating in the 2.4 GHz band should be avoided in densely populated areas due to congestion. The number of wireless LAN access points visible at an arbitrary point in a dense urban area seems to support this evidence. Anyone attending a technology-oriented conference has probably experienced problems connecting to the wireless LAN running on the 2.4 GHz band. Many people now choose to depend on other wireless technologies operating in licensed bands (e.g. mobile 3G and LTE) for connectivity at such events.

Fig. 1. Photograph of the device used to perform measurements.

With our survey we wanted to obtain an up-to-date picture of the situation in the 2.4 GHz band. We performed measurements specifically in environments where we have heard complaints about wireless services. We wanted to verify how much truth is in claims that such problems are related to the over-usage of the spectrum.

Due to a relatively long duration of this study, we wanted to avoid occupying expensive laboratory equipment for its whole duration. The nature of the study also favored a small, easily portable and robust measurement setup. We have therefore constructed a low-cost spectrum sensing device based on a wireless sensor node specifically for these measurements.

Our contribution is therefore twofold: we provide an updated picture of the situation in the 2.4 GHz band in in-door environments and assess the feasibility of using a low-cost sensor node to perform such measurements.

In Section II we give a description of our sensing device and characterization measurements we performed to verify that it is working correctly. Next we describe methods used to analyze collected data in Section III. We describe the channel occupancy criterion and plots used to present the results of our measurement campaigns. Measurement locations are listed in Section IV. Finally, we present results of our study in graphical form in Section V and conclude with Section VI.

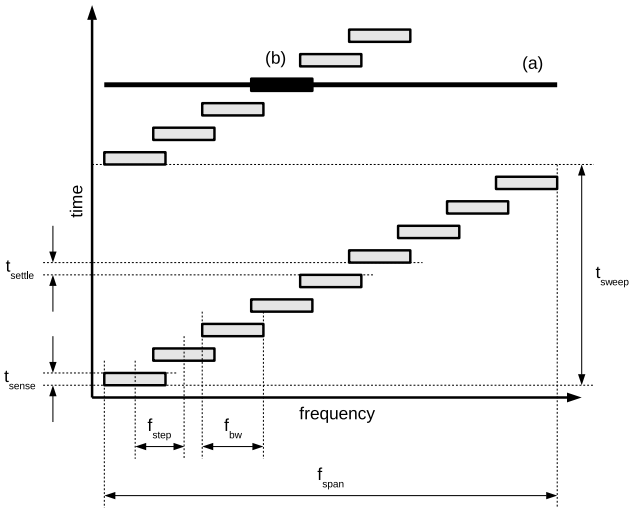

Fig. 2. Definition of sensing parameters. Short, wide-band transmissions (a) are typically detected only as a single occupied channel (b).

II. Equipment

To perform the measurements, we built a stand-alone measurement device shown in Fig.1. The device is based on the VESNA sensor node with a SNE-ISMTV-2400 expansion[5] mounted in a plastic box. During measurements the device was powered by an external 12 V power supply from the AC power grid. A 2 GB micro SD card was used to store data.

Firmware on the sensor node controlled the radio and stored channel RSSI samples onto the SD card. A simple append-only binary format was used. After each completed frequency scan, a record containing a timestamp, an array of power samples and a CRC32 digest was written to the card. For the long-term measurement campaign, when the capacity of a single SD card did not suffice to store a complete record of the campaign, the device was periodically powered off for a short time and SD card manually replaced.

No real-time clock was implemented on the node. Measurements commenced immediately after the node was powered up and timestamps were relative to the time of power up. Firmware accounted for the possibility of power loss during the measurement campaign and continued the binary log at the point of interruption, albeit starting again at timestamp zero. To make it possible to convert relative timestamps to wall-clock time, the time and date of the start of each measurement campaign were noted manually.

A Linx Technologies ANT-2.4-CW-CT 2.4 GHz half-wave dipole antenna was used to receive the radio signals. Antenna was oriented vertically during the measurements and was hence most sensitive to vertically polarized signals. Its peak gain is specified by the manufacturer as 2.8 dBi[6]. Antenna was mounted on a connector that passed through the top of the box and was connected to the radio on the sensor node using a short length of a coaxial cable.

TABLE I
Values of spectrum sensing parameters

parameter	value	
$t_{settle} + t_{sense}$	1.13	ms
t_{sweep}	288	ms
f_{step}	399.628	kHz
f_{BW}	421.875	kHz
$N_{channels}$	255	

A. Spectral power density measurement method

Spectral power density was estimated using the RSSI functionality of the Texas Instrument CC2500 transceiver[7] on the SNE-ISMTV-2400 expansion board. The radio configuration used divided the 100 MHz of spectrum between 2.4 and 2.5 GHz into 255 discrete channels, each approximately 400 kHz wide. The radio hardware allows for measurement of signal power in a channel with a logarithmic scale and resolution of 0.5 dBm.

To estimate power spectral density for the complete band, the transceiver was consecutively tuned to each channel, starting at channel 0 at 2.4 GHz and increasing to channel 254. On each channel, 10 RSSI measurements were taken and averaged in the linear scale to obtain one power sample. After sampling all 255 channels, the procedure was repeated.

The scanning pattern is illustrated in Fig.2. Corresponding parameter values are given in Table I. Each frequency scan resulted in a 518 byte record, resulting in approximately 13 days of autonomy using a 2 GB card.

It should be noted that this specific scanning pattern introduces some artifacts. Firstly, broadband transmissions with the duration significantly shorter than t_{sweep} and bandwidth larger than f_{BW} typically only show up on one power sample in our measurements. A common example observed is an idle IEEE 802.11b/g/n access point. The access point in this case regularly transmits beacon broadcasts, which are short transmissions with approximately 20 MHz bandwidth. A common beacon period is 100 ms. Such an access point appears in our measurements as individual power samples with a high value inside the 20 MHz band.

Secondly, our spectrum sensor has some blind time t_{settle} after a channel change. Transceiver documentation states that the channel hop time with the configuration used by our firmware is approximately 720 microseconds and is dominated by the phase-locked loop calibration time. It is not clear however how this time is related to the blind time for RSSI sampling. We have only directly measured t_{sweep}. From the results of our measurements it appears unlikely that the power detector is blind during the complete calibration period, as that would mean that blind time accounts for approximately 63% of the measurement period.

Another unknown is the relationship between detector output and transmission power for short transmissions with time less than t_{sense}. Our analysis of the data assumes that a max-hold detector is used by the transceiver (i.e. it returns maximum power encountered during sensing time), but it is

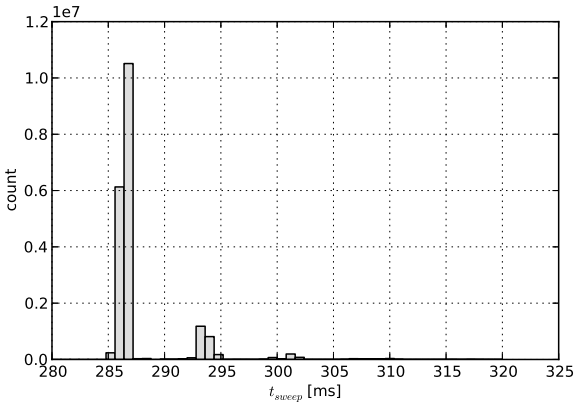

Fig. 3. A histogram of observed t_{sweep} values.

likely that short transmissions registered a lower than actual power with our device.

CPU on the sensor node was tasked with both controlling the radio and writing data to the SD card. No real-time scheduling scheme was used, which led to an uncertainty in t_{sweep}. While the average t_{sweep} was 288 ms, individual sweeps took up to 320 ms. A histogram of frequency sweep times is shown in Fig.3.

B. Characterizing the spectrum sensor

The *vesna_rftest* utility from the *vesna-spectrum-sensor*[1] package was used to characterize the specific device used for measurements. For these measurements, the antenna on the device was replaced with a short length of a low-loss coaxial cable connected to a Rohde & Schwarz SMBV100A signal generator. The effect of the coaxial cable between the antenna connector and the radio circuit board is therefore included in these measurements.

Detector response to different continuous-wave power levels on the antenna connector is shown in Fig.4. It can be seen that the detector has good linearity for input powers up to around -25 dBm. As expected, detector response asymptotically approaches the noise power when the input signal power is decreased below -80 dBm.

Frequency dependence of the detector response is shown in Fig.5. It can be seen that measurement error due to changing sensitivity of the detector is below 1 dB in the measured band.

Finally, the measured shape of the channel filter characteristic is shown in Fig.6. It can be seen that there is some overlap between the adjacent channels, as was expected from the values for f_{step} and f_{BW} given by the manufacturer.

To characterize the internal noise floor of the receiver, a calibration measurement campaign with approximately 300.000 frequency sweeps was performed where the antenna was replaced by a 50 ohm terminator.

[1]https://github.com/sensorlab/vesna-spectrum-sensor

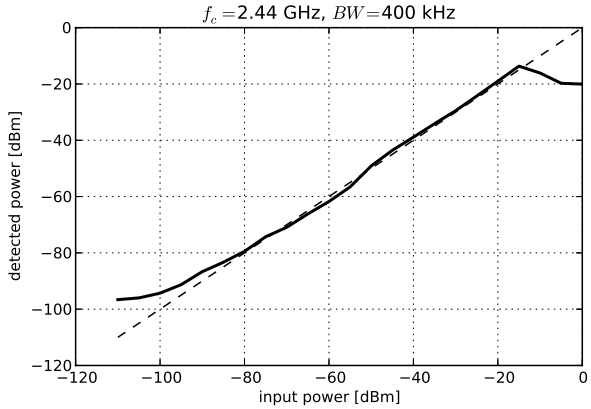

Fig. 4. Detected power versus calibrated input power for the receiver used. Dotted line shows ideal characteristic.

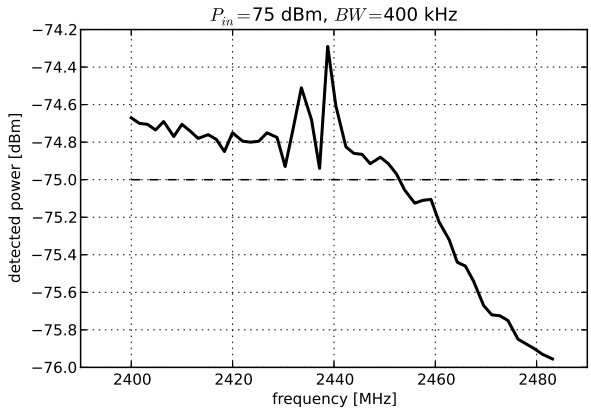

Fig. 5. Detected power versus frequency with constant input power for the receiver used. Dotted line shows ideal characteristic.

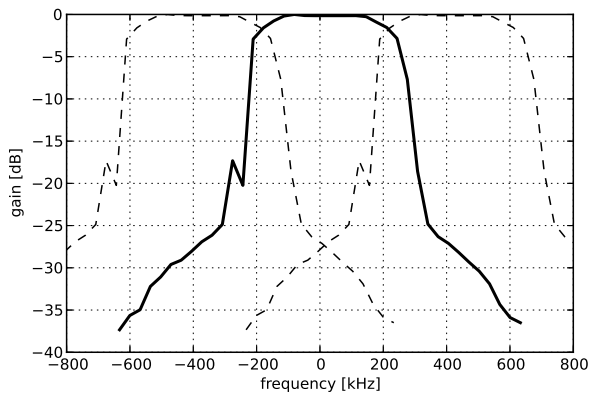

Fig. 6. Bold line shows filter gain for the tuned channel. Dotted lines show gains for adjacent channels.

III. Data analysis methods

A. Threshold selection

The analysis of recorded measurements required a method of determining whether a part of the spectrum is occupied or vacant. Since our spectrum sensor only recorded information about total power in a channel, the only occupancy decision method available was energy detection. In an energy detector, a channel is deemed occupied if detected power is higher than a predetermined threshold and vacant otherwise.

Several methods for determining the threshold are listed in the literature[8]. For our analysis we chose the fixed probability of false alarm (P_{fa}) method, as we consider it the most well-defined from a mathematical point of view.

We determined the energy detection threshold γ_0 using the CCDF method[9] on the calibration measurement campaign. The probability of false alarm was chosen as $P_{fa} = 0.99$. Fig.7 illustrates application of this method on one of the frequency channels.

The estimated threshold for each frequency channel can be seen in Fig.8. The threshold shows some variation versus frequency. Considering that we did not see much variation in detector sensitivity this is unexpected.

Spikes in noise power that repeat every 13.5 MHz are most likely a spurious signal from the 27 MHz crystal oscillator that serves as a reference for the PLL. The predicted harmonics of the half of the crystal resonant frequency are shown as dotted lines in Fig.8 and match the observed data perfectly.

We attributed the increased noise around 2.417 and 2.437 MHz to the reception of the signal from a local IEEE 802.11g network on channels 2 and 6. The calibration campaign was not performed in an anechoic chamber, so it is possible that some of the radiation on these frequencies was received by our receiver despite the fact that the input was terminated without an antenna. It seemed prudent to ignore this interference in the determination of the threshold.

Given these considerations, we have decided to use a constant threshold value for all channels. Final value for γ_0 was calculated from channels that did not show interference during the measurement campaign.

$$\gamma_0 = -98.0\text{dBm} \tag{1}$$

It should be noted that due to the nature of our γ_0 estimation, the channel occupancy statistics that resulted from our analysis should be considered only an upper bound to real occupancy.

Firstly, we have chosen to ignore internal interference from the transceiver's crystal oscillator. For those channels the probability of false alarm must have been higher than the chosen value for P_{fa}.

Secondly, in our calculation of the threshold we have not considered any environmental noise at these frequencies. Since our calibration measurement campaign was performed using a passively terminated antenna connector, only thermal noise and noise sources internal to the transceiver were accounted for. Therefore even in an environment with no legitimate transmissions in the 2.4 GHz band, the real probability of false alarm would likely be higher than the chosen value.

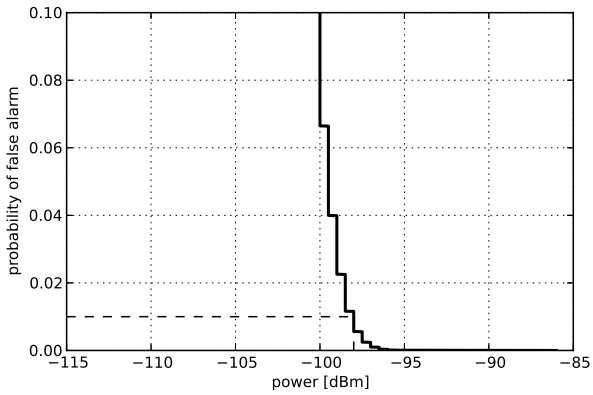

Fig. 7. Determining the energy detection threshold at 2.48 GHz using the complementary cumulative distribution function method.

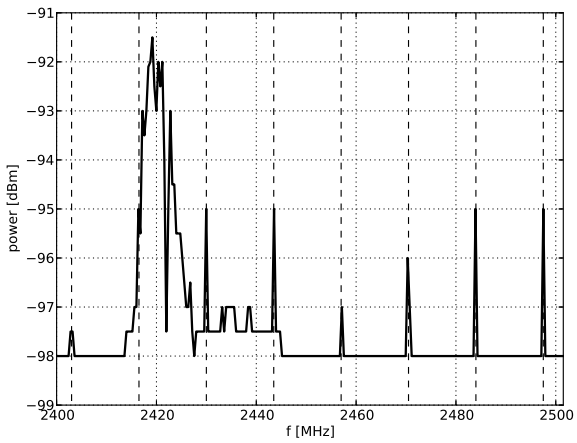

Fig. 8. Bold line shows energy detection threshold versus frequency. Dotted lines mark harmonics of the crystal oscillator.

We have also ignored any changes in the transceiver internal noise sources due to changes in temperature.

To place our value of detection threshold in context, Table II shows a few typical receive sensitivities of IEEE 802.11g transceivers. When accounting for the difference in measurement bandwidth (20 MHz for a 802.11g channel versus 400 kHz channel in our measurements) it can be seen that the weakest decodable wireless LAN signals are just barely detectable using our equipment. Theoretically, a constant-wave transmission at that power would have around 4% probability of detection on our device. For comparison, a -99 dBm signal has around 80% probability of detection.

B. Channel occupancy statistics

In analyzing spectral power densities in the context of spectrum occupancy statistics we followed standard practices[3].

TABLE II
TYPICAL RECEIVE SENSITIVITIES OF 802.11G TRANSCEIVERS. FIGURES GIVEN ARE FOR 6 MBPS MODE AND 10% PACKET ERROR RATE (WHERE SPECIFIED).

model	year	sensitivity [dBm]	
		20 MHz	400 kHz
D-Link DWL-2100 AP[10]	2004	-87	-104
Cisco Aironet CardBus[11]	2007	-86	-103
Advantech EKI-6311GN[12]	2010	-89	-106

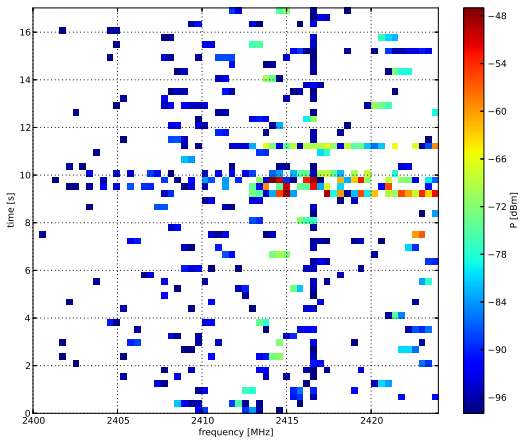

Fig. 9. A detail of a waterfall plot in Fig.16c.

For each measurement campaign, the following statistics were calculated:

1) Max-hold plot: Max-hold plot shows the maximum power seen in each channel for the duration of the measurement campaign. It typically shows the signal strength from the strongest transmitter on the channel that was in operation during the campaign.

2) Channel occupancy plot: Channel occupancy plot shows fraction of time (also called the duty-cycle) each frequency channel was occupied. Value of 1 means the channel was constantly occupied during the measurement campaign.

3) Waterfall plot: The waterfall plot shows detected power versus time and frequency. Points where the signal power is below the threshold are shown in white.

It should be noted however that waterfall plots as shown here can give a false impression that most of the spectrum is constantly occupied. This is a consequence of the way plots are drawn. Since the number of scans on the time axis is significantly larger than the resolution of the plot, several power samples must be shown as a single point. The point color is determined by the maximum power sample covered by that point. Hence even if only one sample is above the detection threshold, the point is shown as occupied. This effect can be seen by comparing Fig.16c with a zoomed-in detail of the same data depicted in Fig.9.

4) Cumulative occupancy plot: This plot shows the fraction of time when more than a certain fraction of the entire frequency band is vacant. For instance, a point on this graph at 95% spectrum vacancy and 40% time fraction means that more than 95% of frequency channels were vacant 40% of the time during the measurement campaign.

5) Fraction of vacant spectrum versus time of day: This plot shows daily variations in the fraction of vacant frequency channels in 15 minute time slots.

6) Compactness of vacant channels versus time: This graph shows the compactness measure of vacant channels. Compactness measure c is defined as[13]:

$$c = \sqrt{\frac{c_2 - c_1}{c_1^2 - c_1}} \tag{2}$$

$$c_1 = \sum_k b_k \tag{3}$$

$$c_2 = \sum_k b_k^2 \tag{4}$$

where b_k is number of contiguous vacant channels in block k. For instance, if all vacant channels are in a single, contiguous block, $c = 1$. If all vacant channels are dispersed in blocks of only one channel, $c = 0$.

IV. LOCATIONS

We performed measurements in Slovenia between April and June 2014 at 5 different residential locations and 1 conference.

It should be noted that occupants of residential locations work in the technology sector and are relatively heavy users of devices with wireless connectivity. For example, the following devices were seen in the vicinity of our spectrum sensing device during the measurement campaigns: multiple laptops, smartphones and tablets with 802.11b/g/n wireless LAN and Bluetooth interfaces, wireless peripherals like keyboards, mice and game controllers using proprietary technologies on the 2.4 GHz band and home theater equipment with wireless video and audio streaming technologies.

Given the above, we consider it likely that these households are above average in 2.4 GHz band usage in Slovenia.

A local wireless LAN access point was installed in all locations, both conference and residential. Because measurements were taken in densely populated areas, a 802.11b/g/n network scan typically also listed 10 - 20 other access points at unknown locations.

Location A was located in a dense residential district of Ljubljana. Measurements were performed in a second floor apartment of a 4 floor apartment block. Two measurement locations, designated A1 and A2, were located in two different rooms of the apartment. Both rooms had windows overlooking more apartment blocks.

Location B was located on the ground floor of a single-family house located outside of the ring road of Ljubljana. The immediate neighborhood consisted of other single- and two-family houses. Measurements were performed in an interior room.

TABLE III
LOCATIONS AND DURATIONS OF MEASUREMENT CAMPAIGNS.

campaign	location	scans	duration	
1	A1	2754631	9 days,	4:22:19
2	A2	2528601	8 days,	10:48:13
3	B	3348882	11 days,	4:35:35
4	C	2539291	8 days,	11:39:11
5	D	2467861	8 days,	5:55:46
6	E	64781		5:11:33
7	A1	19775893	66 days,	3:49:48

Location C was located in a residential district in Ljubljana, different from Location A. Measurements were performed in a second floor apartment in a larger apartment complex.

Location D was located in a two-family house in a suburban residential area outside of Ljubljana.

Location E was in the main hall of the University of Ljubljana, Faculty of Electrical Engineering, during a one-day Webcamp Ljubljana conference. The conference was focused on web technologies and had approximately 200 attendees. Most brought a laptop and a smartphone with them.

For all locations, the data collection period was about 10 days, limited by the capacity of the SD card used for storing spectral power density data. Two exceptions being location E, where data collection was limited to the duration of the conference event, and location A1 where data collection was performed for around 2 months. Exact duration and the total number of frequency sweeps for each campaign is shown in Table III.

V. RESULTS

Results of short-term campaigns are shown in Fig.10, 11, 12, 13, 14 and 15. Results of the long-term campaign are shown in Fig.16.

Channel occupancy plots show that the 2.4 GHz band is surprisingly vacant. Even though our measurement method likely overestimated the spectrum occupancy, most locations had overall occupancy well below 15%. Only the Webcamp conference had a significantly higher percentage of occupied channels, but even then the occupancy did not reach 50%. As expected, frequency channels with spurious emissions from the local oscillator are shown with a significantly higher occupancy due to their higher false alarm rate.

The compactness measure for vacant channels is between 0.4 and 0.6. For comparison, vacant spectrum blocks of 20 MHz would result in approximately $c = 0.5$.

It is possible that this result is not accurate. Sensor blind time, which is unknown for our device, could have caused our sensor to miss a non-negligible portion of short transmissions. However due to sampling theorem and the fact that our detector was not synchronized with any transmitter, we consider it unlikely that this would significantly affect the average occupancy value. An unfavorable detector duty cycle characteristic (another unknown in our case) would be another possible cause that our results underestimate occupancy.

On the other hand, other less focused studies have seen similar low figures for the 2.4 GHz ISM band in the past. For instance, occupancy of 2.4 GHz band in Paris and Brno in 2008 and 2009 was found to be less than 10%[2]. Occupancy of around 25% was seen in Chicago and New York in 2006[1]. Some of these studies attributed the low occupancy of this band to their out-doors measurement location, away from any users of the band. However if our results are accurate, they would suggest that the band is in fact not significantly congested most of the time.

Given these results it is difficult to explain the poor performance of wireless LAN (we have experienced connectivity problems at the Webcamp conference ourselves). It is possible that even with such a low average utilization of the medium, physical and MAC layers exhibit poor performance. For example, it might be that while the overall utilization of the spectrum was low, individual vacant timeslots were short. We have not performed accurate time-domain analysis to confirm this. Slow frequency sweep of our device would make the value of such results questionable at best.

Even though our sensor was less sensitive compared to typical wireless LAN interfaces, we consider it unlikely that this significantly affected our results in the context of wireless LAN interference. Connectivity problems reported were always in relation to a local access point. Very weak transmissions we might have missed should not cause much interference in that case.

We have also observed variations in spectrum occupancy in relation to the time of day. This confirms the assumption that this frequency band is mostly used by consumer devices. As expected from a typical network where significant traffic is human-to-human or human-to-machine, the occupancy drops during night time. However we have also seen some evidence of scheduled machine-to-machine communication. For example, it is unlikely that regular drop in vacant spectrum in Fig.10e between 1:00 AM and 3:00 AM is due to user activity.

VI. CONCLUSIONS

In this paper we have presented spectrum occupancy estimates from 7 measurement campaigns performed in in-door environments. According to our study, more than 90% of spectrum is available more than 95% of the time in residential areas in Ljubljana, Slovenia. Daily variations in occupancy exist, but are limited to approximately 2%. In a conference environment, overall occupancy reached at most 40%.

While some possibilities exist that our results have under reported the occupancy, our results agree well with previous studies and are more likely to have overestimated occupancy. We have also shown that a robust sensor node can be used to perform spectrum occupancy studies with a reasonable accuracy given previous characterization with calibrated equipment. Several possible drawbacks of our spectrum sensor were identified during the measurement which should be addressed in further work using this hardware.

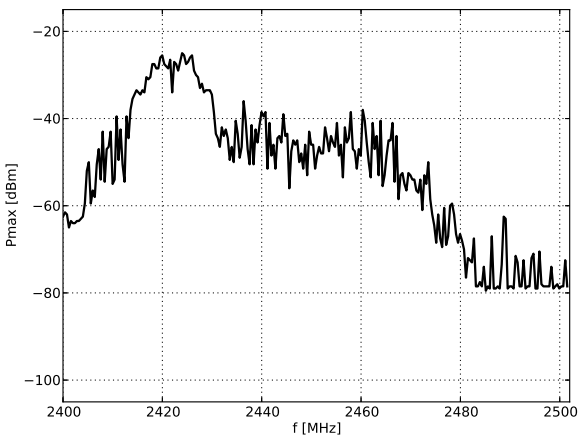

(a) Maximum power observed at each frequency channel.

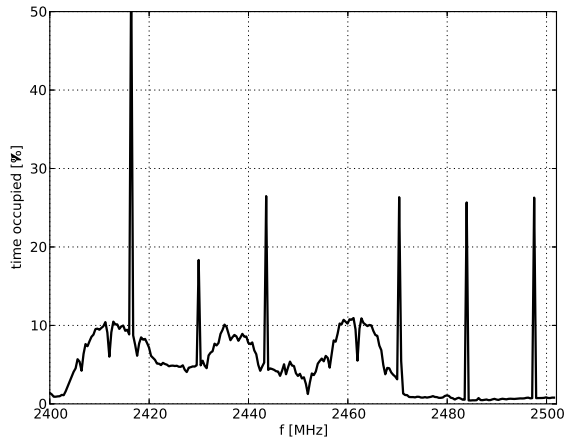

(b) Fraction of time each frequency channel was occupied.

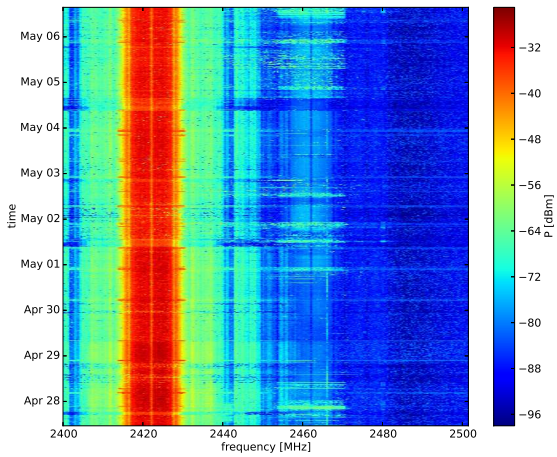

(c) Waterfall plot

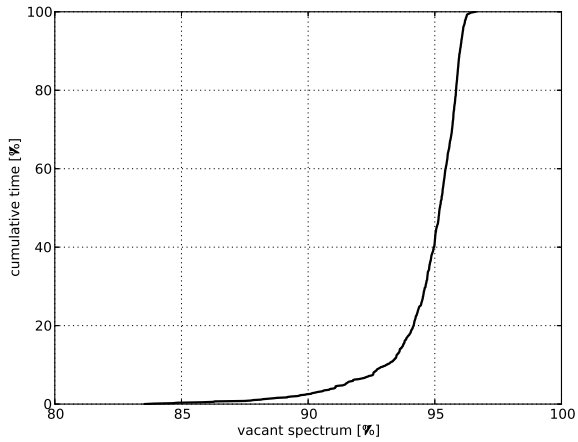

(d) Cumulative fraction of time versus total spectrum occupancy.

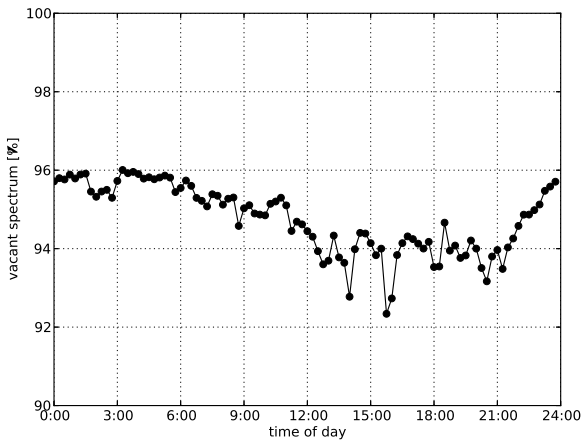

(e) Percentage of vacant frequency channels versus time of day.

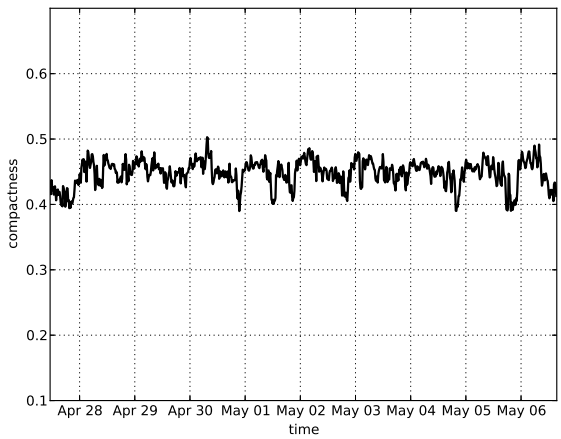

(f) Compactness of vacant channels versus time.

Fig. 10. Results for location A1 (urban, residential).

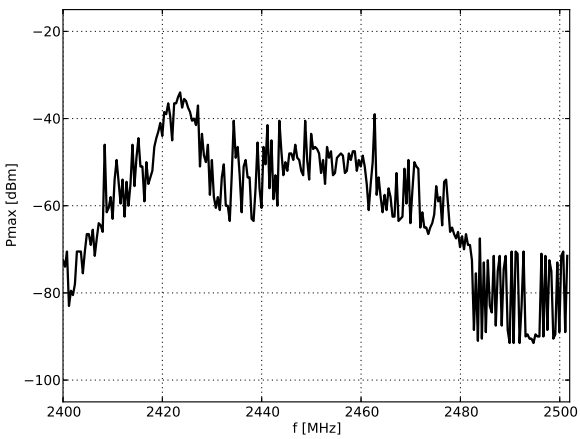

(a) Maximum power observed at each frequency channel.

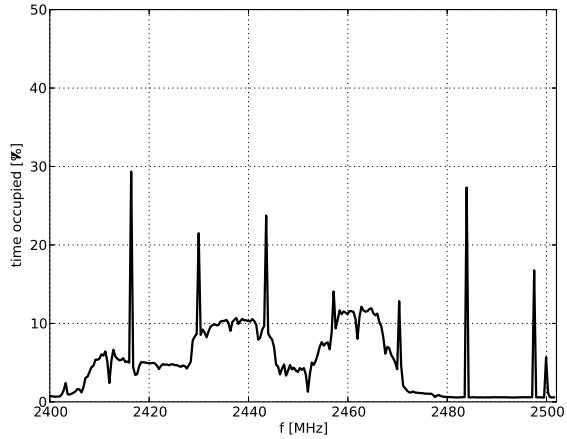

(b) Fraction of time each frequency channel was occupied.

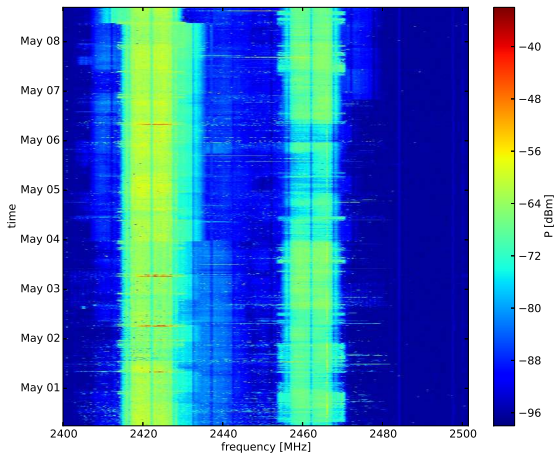

(c) Waterfall plot

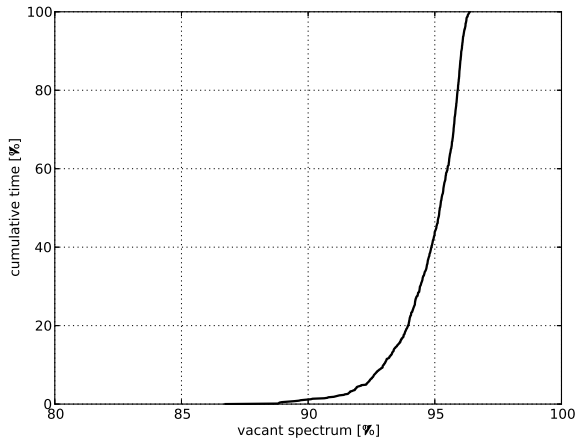

(d) Cumulative fraction of time versus total spectrum occupancy.

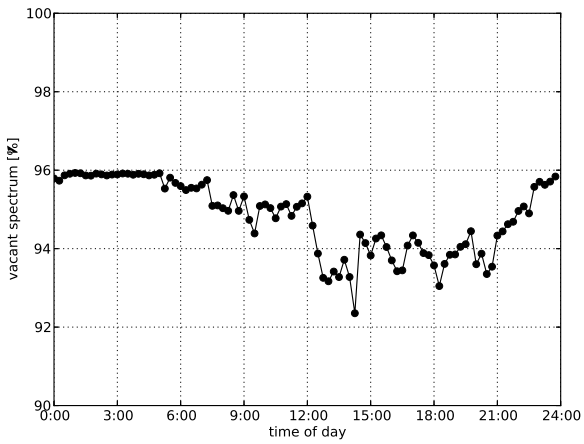

(e) Percentage of vacant frequency channels versus time of day.

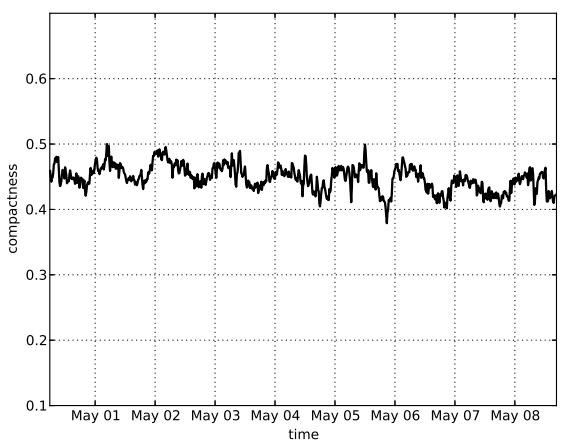

(f) Compactness of vacant channels versus time.

Fig. 11. Results for location A2 (urban, residential).

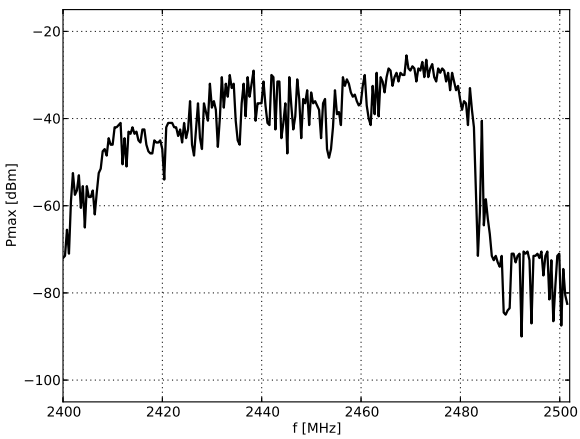

(a) Maximum power observed at each frequency channel.

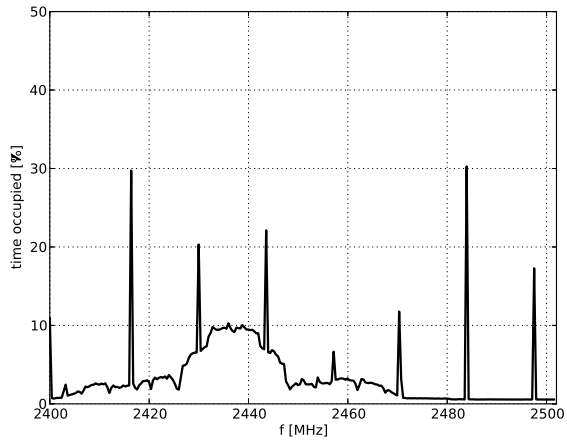

(b) Fraction of time each frequency channel was occupied.

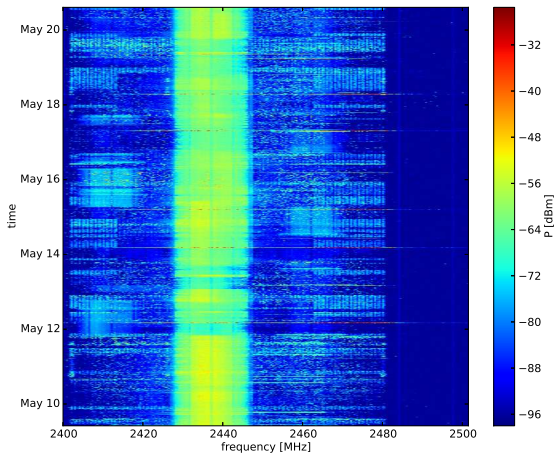

(c) Waterfall plot

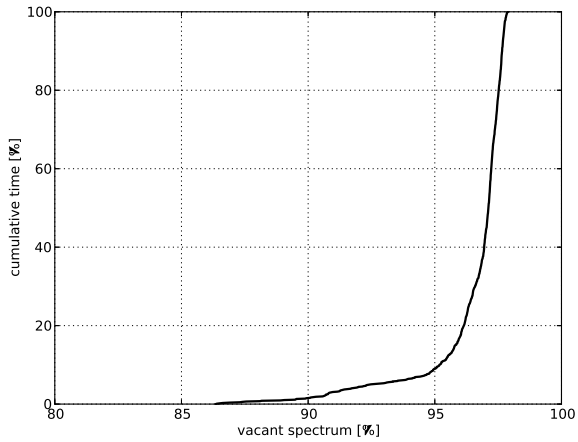

(d) Cumulative fraction of time versus total spectrum occupancy.

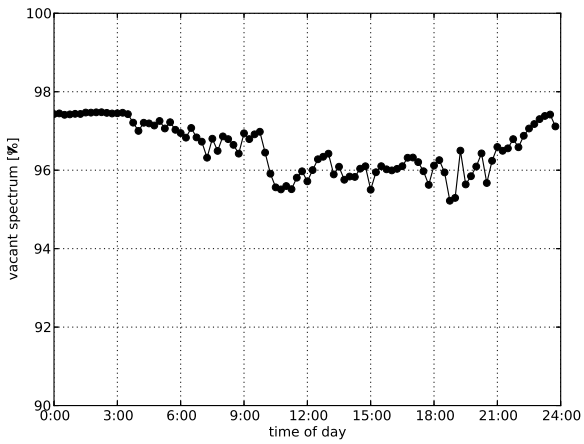

(e) Percentage of vacant frequency channels versus time of day.

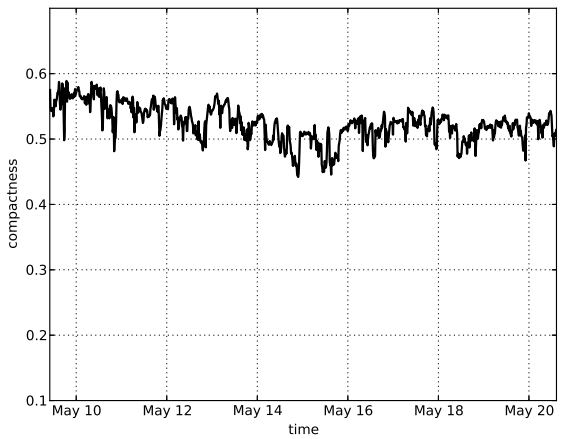

(f) Compactness of vacant channels versus time.

Fig. 12. Results for location B (urban, residential).

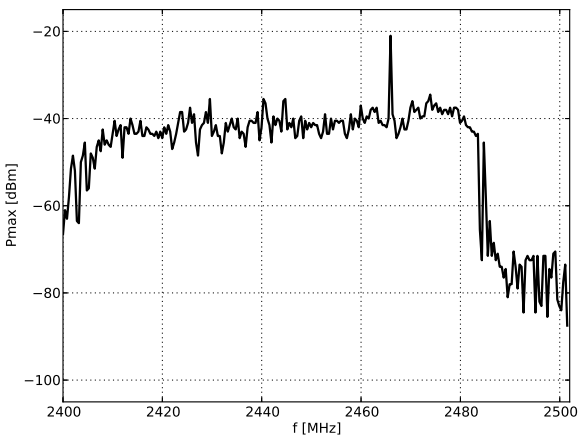

(a) Maximum power observed at each frequency channel.

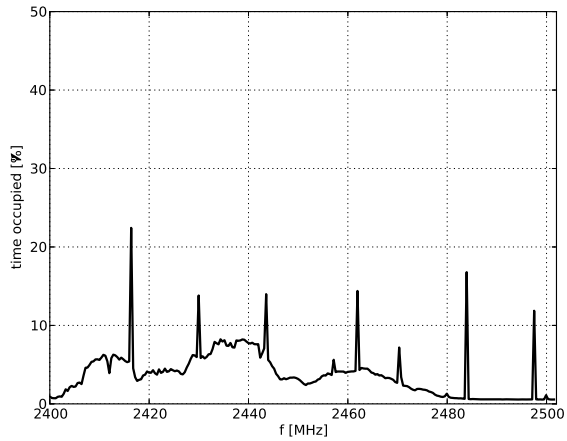

(b) Fraction of time each frequency channel was occupied.

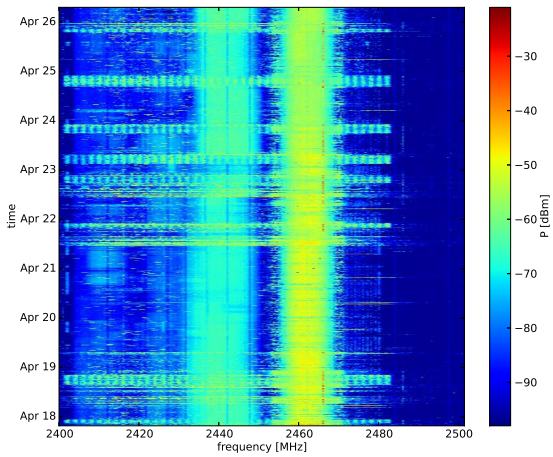

(c) Waterfall plot

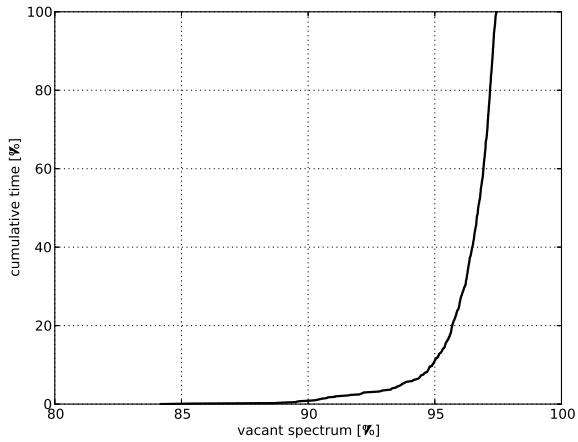

(d) Cumulative fraction of time versus total spectrum occupancy.

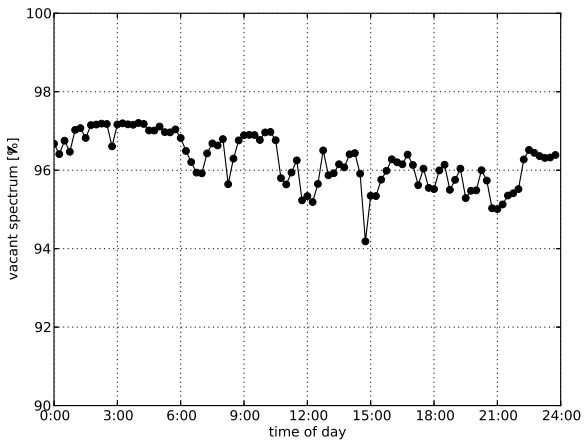

(e) Percentage of vacant frequency channels versus time of day.

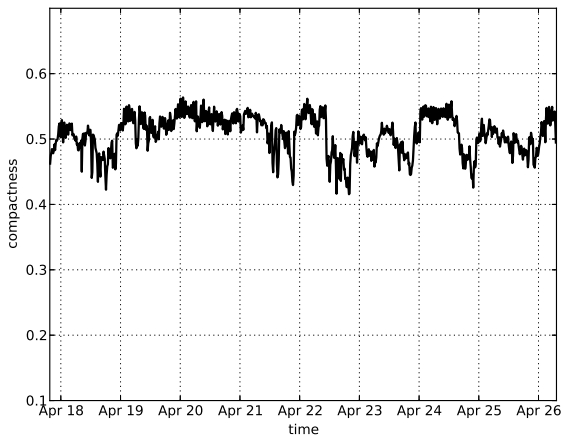

(f) Compactness of vacant channels versus time.

Fig. 13. Results for location C (urban, residential).

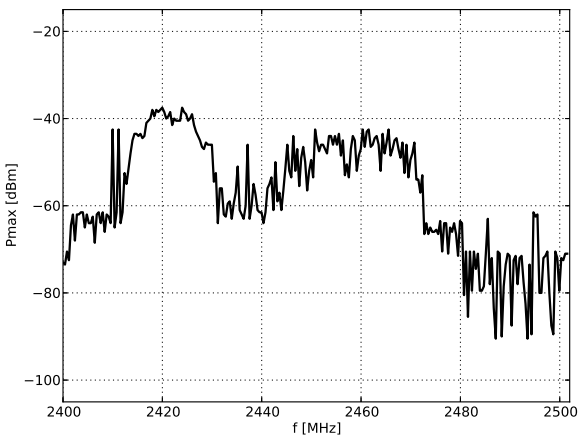

(a) Maximum power observed at each frequency channel.

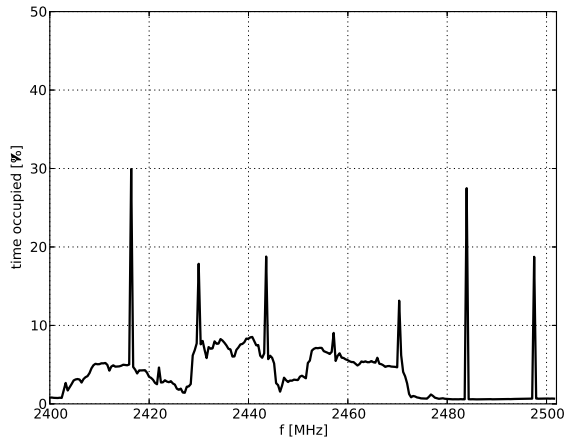

(b) Fraction of time each frequency channel was occupied.

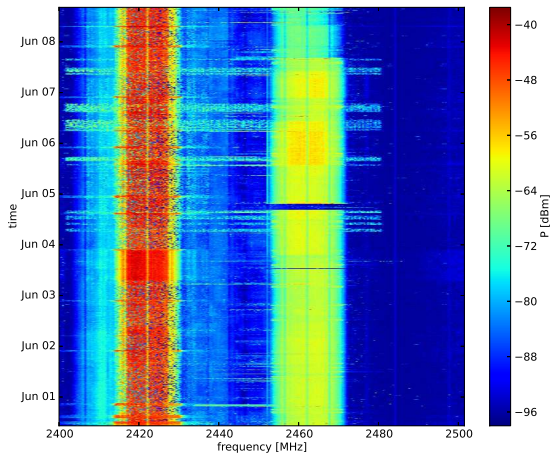

(c) Waterfall plot

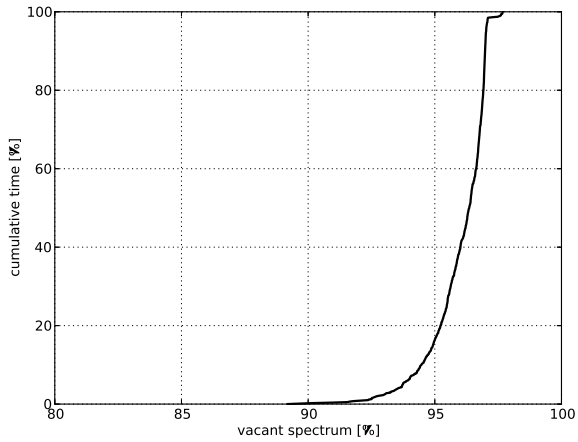

(d) Cumulative fraction of time versus total spectrum occupancy.

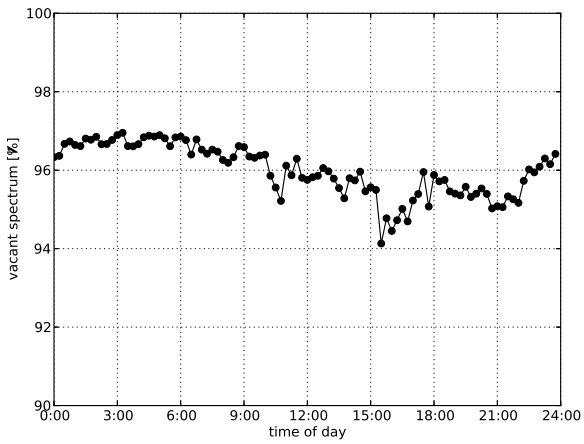

(e) Percentage of vacant frequency channels versus time of day.

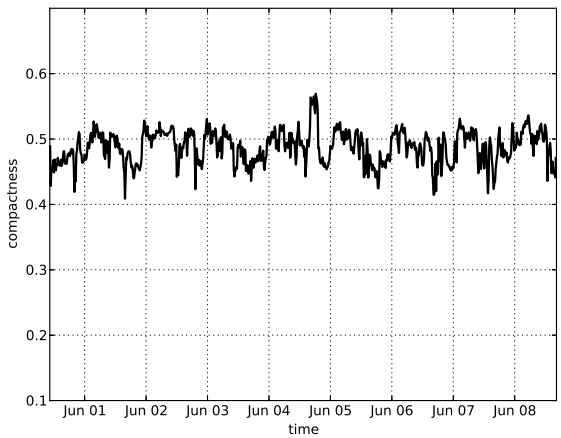

(f) Compactness of vacant channels versus time.

Fig. 14. Results for location D (suburban, residential).

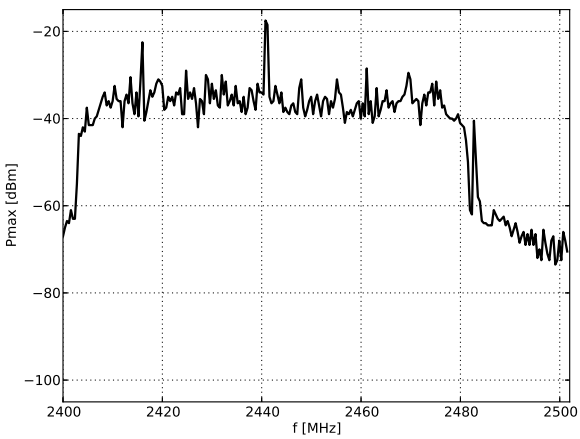

(a) Maximum power observed at each frequency channel.

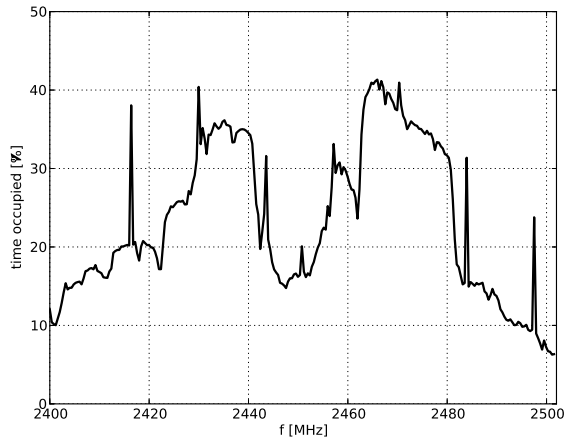

(b) Fraction of time each frequency channel was occupied.

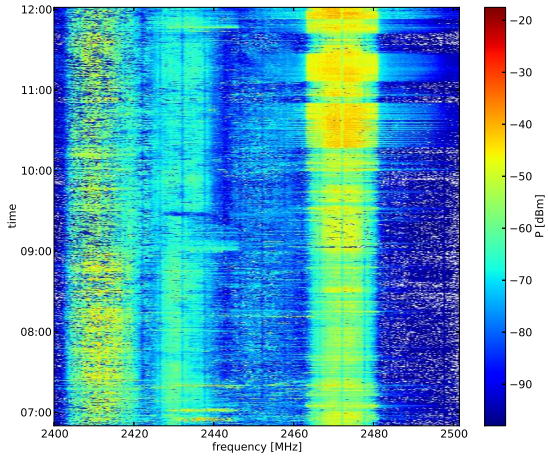

(c) Waterfall plot

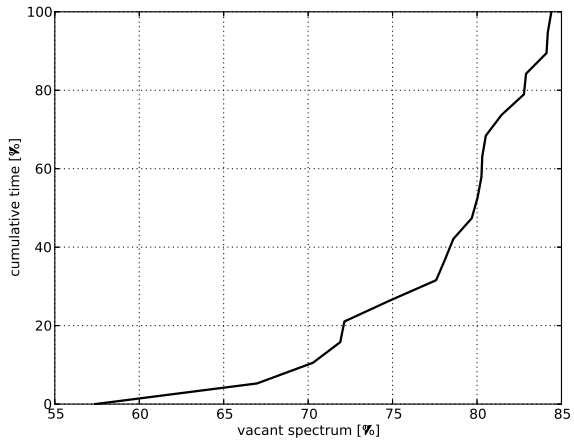

(d) Cumulative fraction of time versus total spectrum occupancy.

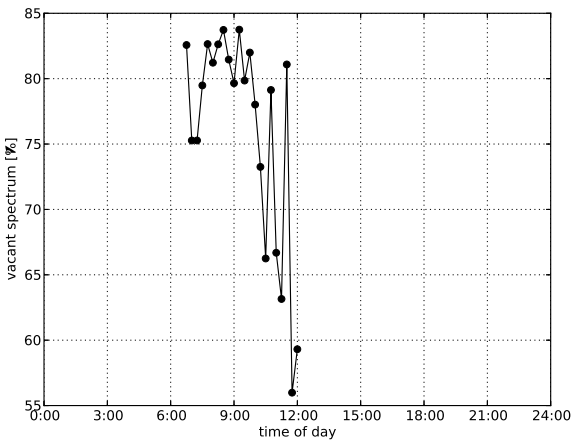

(e) Percentage of vacant frequency channels versus time of day.

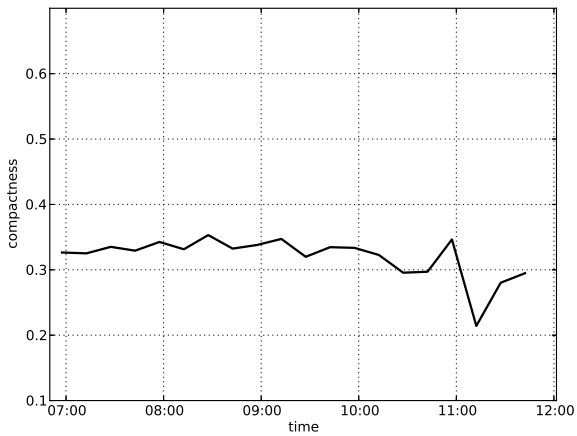

(f) Compactness of vacant channels versus time.

Fig. 15. Results for location E (conference).

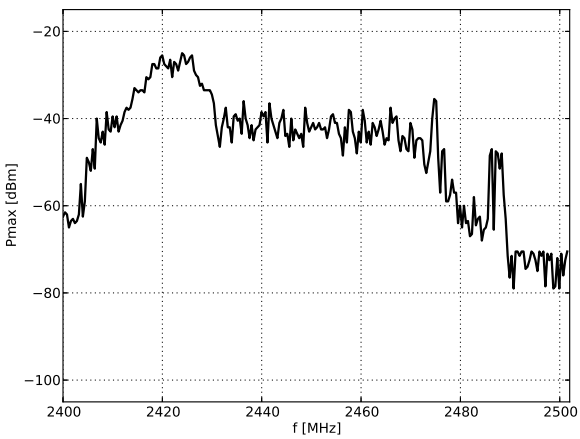

(a) Maximum power observed at each frequency channel.

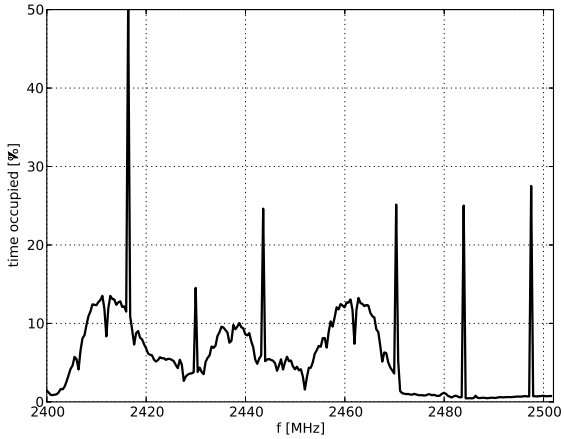

(b) Fraction of time each frequency channel was occupied.

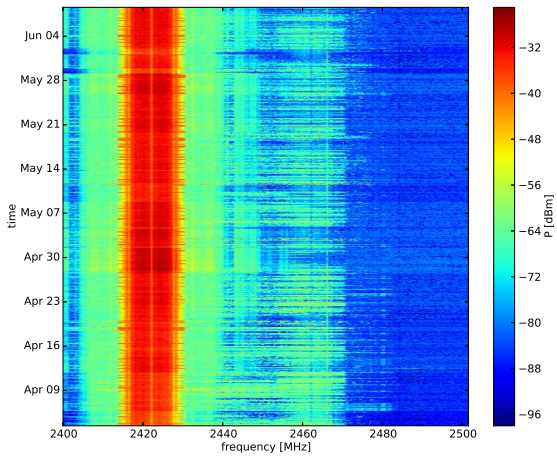

(c) Waterfall plot

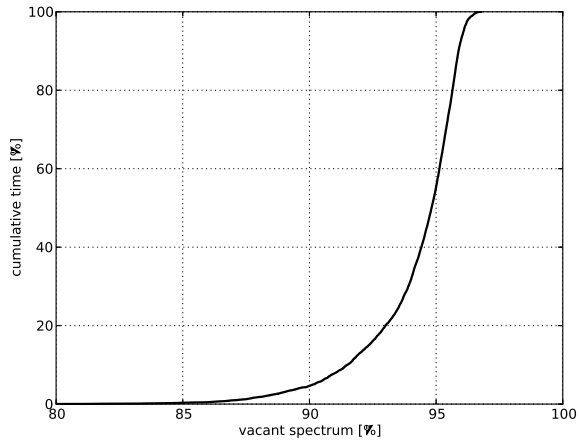

(d) Cumulative fraction of time versus total spectrum occupancy.

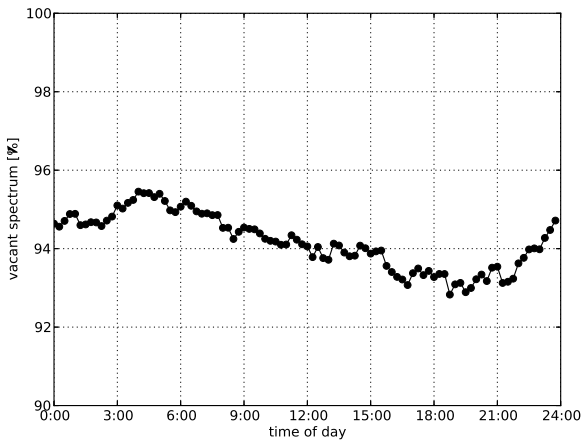

(e) Percentage of vacant frequency channels versus time of day.

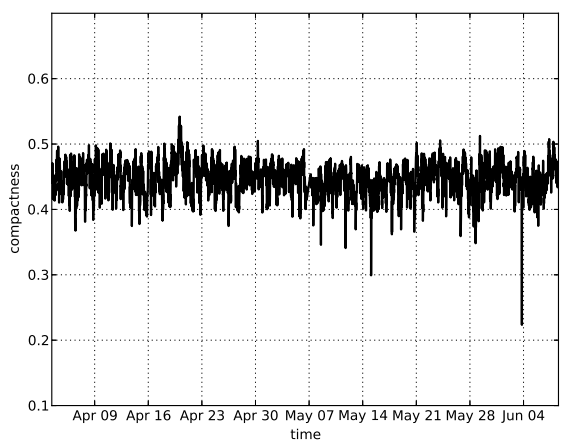

(f) Compactness of vacant channels versus time.

Fig. 16. Results for location A1 (urban, residential).

REFERENCES

[1] M. A. McHenry, P. A. Tenhula, D. McClosky, D. A. Roberson, and C. S. Hood, "Chicago Spectrum Occupancy Measurements & Analysis and a Long-term Studies Proposal," in *First International Workshop on Technology and Policy for Accessing Spectrum*, 2006.

[2] V. Valenta, R. Marsalek, G. Baudoin, M. Villegas, M. Suarez, and F. Robert, "Survey on spectrum utilization in Europe: Measurements, analyses and observations," in *Proceedings of the Fifth International Conference on Cognitive Radio Oriented Wireless Networks & Communications*, pp. 1–5, IEEE, 2010.

[3] Shared Spectrum Company, "General Survey of Radio Frequency Bands - 30 MHz to 3 GHz," 2010.

[4] M. Biggs, A. Henley, and T. Clarkson, "Occupancy analysis of the 2.4 GHz ISM band," *IEE Proceedings-Communications*, vol. 151, no. 5, pp. 481–488, 2004.

[5] T. Šolc, "SNE-ISMTV: VESNA wireless sensor node expansion for cognitive radio experiments," in *Proceedings of the Tenth International Symposium on Wireless Communication Systems*, VDE, 2013.

[6] Linx Technologies, "ANT-2.4-CW-CT-xxx Data Sheet," 2013.

[7] Texas Instruments, "CC2500 Single Chip Low Cost Low Power RF Transceiver," 2006. rev. 1.2.

[8] M. López-Benítez and F. Casadevall, "Methodological aspects of spectrum occupancy evaluation in the context of cognitive radio," *European Transactions on Telecommunications*, vol. 21, no. 8, pp. 680–693, 2010.

[9] R. Dionísio *et al.*, "Sensing algorithms for TVWS operations," public deliverable, COGEU project (FP7 ICT-2009.1.1), 2011.

[10] D-Link, "DWL-2100AP 802.11g High-Speed Wireless Access Point," 2004. rev. 01.

[11] Cisco Systems, "Cisco Aironet 802.11A/B/G Wireless CardBus Adapter," 2007.

[12] Advantech, "EKI-6311GN IEEE 802.11 b/g/n Wireless Access Point/Client Bridge," 2010.

[13] R. Dionísio *et al.*, "Final report on experiment results and user experience," public deliverable, CREW project (FP7 ICT-2009.1.6), 2014.